



# Improved Alignment of PEDOT:PSS Induced by *in-situ* Crystallization of “Green” Dimethylsulfone Molecules to Enhance the Polymer Thermoelectric Performance

Qiang Zhu<sup>1</sup>, Erol Yildirim<sup>2</sup>, Xizu Wang<sup>1</sup>, Xiang Yun Debbie Soo<sup>1</sup>, Yun Zheng<sup>1</sup>, Teck Leong Tan<sup>2</sup>, Gang Wu<sup>2</sup>, Shuo-Wang Yang<sup>2\*</sup> and Jianwei Xu<sup>1,3\*</sup>

<sup>1</sup> Institute of Materials Research and Engineering, A\*STAR (Agency for Science, Technology and Research), Singapore, Singapore, <sup>2</sup> Institute of High Performance Computing, A\*STAR (Agency for Science, Technology and Research), Singapore, Singapore, <sup>3</sup> Department of Chemistry, National University of Singapore, Singapore, Singapore

## OPEN ACCESS

### Edited by:

Sumeet Walia,  
RMIT University, Australia

### Reviewed by:

Ayaskanta Sahu,  
New York University, United States  
Syed Mubeen Jawahar Hussaini,  
The University of Iowa, United States

### \*Correspondence:

Shuo-Wang Yang  
yangsw@ihpc.a-star.edu.sg  
Jianwei Xu  
jw-xu@imre.a-star.edu.sg

### Specialty section:

This article was submitted to  
Nanoscience,  
a section of the journal  
Frontiers in Chemistry

Received: 14 July 2019

Accepted: 30 October 2019

Published: 15 November 2019

### Citation:

Zhu Q, Yildirim E, Wang X, Soo XYD, Zheng Y, Tan TL, Wu G, Yang S-W and Xu J (2019) Improved Alignment of PEDOT:PSS Induced by *in-situ* Crystallization of “Green” Dimethylsulfone Molecules to Enhance the Polymer Thermoelectric Performance. *Front. Chem.* 7:783. doi: 10.3389/fchem.2019.00783

Dimethylsulfone (DMSO<sub>2</sub>), a small organic molecule, was observed to induce the alignment of poly(3,4-ethylenedioxythiophene): poly(4-styrenesulfonate) (PEDOT:PSS) via *in-situ* crystallization in PEDOT:PSS mixture, which was verified by field emission scanning electron microscopy (FESEM), X-ray diffraction (XRD) and atomic force microscopy (AFM). A chemically stable dopant, DMSO<sub>2</sub>, remarkably raised the electrical conductivity of the PEDOT:PSS film, which was fabricated from pre-mixed solution of PEDOT:PSS and DMSO<sub>2</sub>, up to 1080 S/cm, and more importantly, such a PEDOT:PSS film showed a long-term humidity stability and it retained near 90% electric conductivity after 60 days, suggesting DMSO<sub>2</sub> is promising for an eco-friendly alternative to replace dimethyl sulfoxide (DMSO), ethylene glycol (EG) and various acids dopants that have been widely employed to dope and post-treat PEDOT:PSS. Pairwise interaction energies and free energy of solvation between PEDOT:PSS and DMSO<sub>2</sub> were calculated by first-principles and molecular mechanics, respectively, revealing the mechanism of DMSO<sub>2</sub> in enhancing the electrical conductivity.

**Keywords:** dimethylsulfone, PEDOT:PSS, thermoelectric, polymer alignment, crystallization

## INTRODUCTION

In the past few decades, we have witnessed great progress on thermoelectric devices due to its capability to directly convert waste heat into electricity. The efficiency of the thermoelectric materials is evaluated via the dimensionless figure-of-merit:  $ZT = S^2\sigma T/\kappa$ , where  $S$ ,  $\sigma$ ,  $T$ , and  $\kappa$  are Seebeck coefficient, electrical conductivity, thermal conductivity and absolute temperature, respectively. Previously, inorganic materials such as Bi<sub>2</sub>Te<sub>3</sub>, BiSb, SiGe, and other metal alloys (Han et al., 2014; Zhao and Tan, 2014) were extensively studied, achieving a commendable  $ZT$  of about 2 (Culebras et al., 2014b). These materials were fabricated into various devices, which were used in niche applications including refrigeration and power generation. Nevertheless, these inorganic materials are intrinsically disadvantaged because of their scarcity on earth, non-flexibility and toxicity, thus limiting their wide application in thermoelectric modules (Hu et al., 2015a). To overcome such drawbacks, conducting polymers (CPs) are currently studied as alternative

TE materials, given their advantages, such as tunable electric conductivity and low thermal conductivity (Choy, 1977; Kim et al., 2013; Park et al., 2013).

The typical CPs that have been widely studied to date include polyacetylene (Kaneko et al., 1993), polypyrrole (PPy) (Kemp et al., 1999), polyaniline (PANI) (Yoon et al., 1995; Mateeva et al., 1998), polythiophene (PTH) (Hu et al., 2013) and poly(3,4-ethylenedioxythiophene):poly(styrenesulfonate) (PEDOT:PSS) (Zhang et al., 2010). The TE performance of CPs are still much lower than their inorganic counterparts due to their intrinsically low electrical conductivity and relatively low Seebeck coefficient (Culebras et al., 2014b; McGrail et al., 2015). Though the electrical conductivity can be enhanced, the Seebeck coefficient usually decreases correspondingly due to the trade-off relationship between them, resulting in a low power factor, termed as  $P = S^2\sigma$  (Yao et al., 2010). Several approaches have been widely investigated to improve TE performance of the CPs, including (1): nanostructuring CPs, (2): hybridization with other nanostructures, including metallic and carbon-based materials and (3): surface modifications or post-treatment. In the first approach, various CP nanostructures, such as PEDOT nanostructures including nanorods, nanofibers, nanotubes (Hu et al., 2015b), and PPy nanotubes (Wu et al., 2014) have been systematically studied. A significant improvement in TE performance has been observed for these CPs-nanostructure composites as compared to the corresponding bulky CPs. However, the synthesis and fabrication of such nanostructures sometimes involve complicated synthesis and disproportionate scale-up, which limits their applications. The second approach has been widely investigated, which takes advantages of each respective component of the hybrid, high electric conductivity or high Seebeck coefficient, to “balance” the composite materials’ properties (Zhang et al., 2010; Moriarty et al., 2013; Xu et al., 2013; Park et al., 2014a). Thus, an optimum power factor can be obtained via higher energy-filtering efficiency through the joint adjunct between nanoparticles and CPs (Choi et al., 2016). The highest ZT obtained so far is about <0.5 and mechanism for the hybrid materials is unfortunately not fully understood due to many challenging factors involved in the complicated system (Zhang et al., 2010; Kumar et al., 2018). The third approach is to tune the surface morphology through various doping approaches or post-treatments. In this approach, PEDOT:PSS has been the dominant CP to be extensively studied with various post-treatments (McGrail et al., 2015; Wei et al., 2015). The main aim for process or treatment is to remove the insulating polymer PSS from PEDOT:PSS. Various organic solvents (DMSO, EG and other chemicals) and inorganic salts have also been widely used to increase its electrical conductivity in a few magnitudes so that the power factor can be significantly increased (Zhang et al., 2010; Culebras et al., 2014a). Post-treatment by immersing the PEDOT:PSS films into EG or acid solution was also studied (Culebras et al., 2014a; Park et al., 2014b). The mechanism is well-studied and the phase separation of PEDOT is observed in several studies (Timpanaro et al., 2004; Crispin et al., 2006). Our previous modeling study also demonstrated that PSS-DMSO interaction was stronger than these in the PEDOT-PSS, PEDOT-DMSO and PSS-PSS interactions. Thus, dissolution of

insulating PSS shells to release PEDOT conducting cores for self-aggregation is the main mechanism for the enhancement of electrical conductivity (Yildirim et al., 2018).

Aligning conducting polymers is a good method to tune carrier transport properties, and thus improve the thermoelectric properties. In order to align polymers, both common template synthesis and post-treatment methods have been investigated. Feng et al. reported the use of electrospinning and oxidative chemical polymerization to feasibly synthesize PEDOT fibers and tubes (Feng et al., 2013). Aligned PEDOT structures can be obtained through the template synthesis, but the whole process of the template synthesis is quite complicated and the template polymer has to be employed and removed in the fabrication. Another example is vapor-phase polymerization, in which an oxidant is used as a template and EDOT monomers stack via a bottom-up approach for well-ordered PEDOT crystals (Kim et al., 2007; Laforgue and Robitaille, 2010). Lee also proposed to post-treat a pre-fabricated PEDOT:PSS film with sulfuric acid. High-angle annular dark-field scanning transmission electron microscopy (HAADF-STEM) and X-ray powder diffraction (XRD) studies revealed that the PEDOT fibril structure was observed, resulting in a remarkably high electrical conductivity (4,380 S/cm). (Kim et al., 2014) Toward this goal, there seems no report using small molecules to induce the PEDOT:PSS polymer alignment. The major challenge of this is that the most commonly used molecules, such as DMSO, EG, acids and hydrazine are liquid which is unable to shape the polymer in a well-oriented way.

In this paper, we first identified a small molecule, dimethylsulfone (DMSO<sub>2</sub>), which is water-soluble and miscible with PEDOT:PSS well. DMSO<sub>2</sub> is able to crystallize from the PEDOT:PSS system and indirectly align PEDOT:PSS through the hydrogen bonding interactions. Such alignment significantly increases electrical conductivity of PEDOT to 1080 S/cm, comparable to DMSO and EG, suggesting that DMSO<sub>2</sub> is a green alternative to replace widely used DMSO and EG for solvent treatment of PEDOT:PSS. Furthermore, DMSO<sub>2</sub> has several advantageous properties in term of non-toxicity, solid and high solubility in water. These properties make DMSO<sub>2</sub> appropriate for wearable electronics devices that are required to direct contact with human skins.

## EXPERIMENT SECTION

### Materials

Microscopic glass slides (25 mm by 75 mm), dimethylsulfone (purity ≥98%) were purchased from Sigma Aldrich. PEDOT:PSS aqueous solution (PH1000, Heraeus Clevis) was purchased from Heraeus, Germany. All other solvents, such as EG, ethanol and distilled water were used as received without further purification.

### Sample Preparation

Glass slides were first pre-treated by immersing in *aqua regia* for 2 days at ambient temperature to enhance its hydrophilic property. The glass slides were further washed consecutively with distilled water, isopropanol, and acetone prior to being dried under air flow. Preparation of 1% DMSO<sub>2</sub> in PEDOT:PSS is used

as an example. Dimethylsulfone (4.0 mg) was added into a 2-mL sample vial containing 400.0 mg of PEDOT:PSS aqueous solution at ambient temperature. The pre-mixed solution was stirred under vortex for 5 min to ensure that DMSO<sub>2</sub> is fully dissolved in PEDOT:PSS prior to ultrasonication for 20 min. The as-prepared solution was loaded onto the 2.5 × 2.5 cm<sup>2</sup> pre-treated glass slide and left to stand for 5 min at ambient temperature. It was then further cured at 80°C for 40 min to obtain a thin film. In some cases, shrinkage was observed during the curing stage at 80°C; a glass pipette can be used to spread the solution so that a uniform film can be prepared.

## Post-treatment

The as-prepared doped PEDOT:PSS film annealed on the glass substrate was immersed in solvents, such as water, methanol and ethanol respectively for 1 h at ambient temperature. The glass substrate together with the film was then carefully taken out and dried over the hotplate at 80°C for 30 min. The corresponding films obtained are then for the electrical conductivity measurements.

## Characterization

The morphologies of the PEDOT:PSS films were studied using field emission scanning electron microscope (FESEM) on JSM6700F and atomic force microscopy (AFM) on Nanoscope IIIa instrument, Digital Instrument. XRD Measurement was performed on PANalytical X'Pert PRO High Resolution XRD. The electrical conductivity of PEDOT:PSS films were measured by Loresta-GP MCP-T600 (Mitsubishi Low Resistivity Meter) at room temperature. The thicknesses of the films were determined with a KLA Tencor P-16+ Surface Profiler. The Seebeck coefficient was measured by the custom-made measurement system equipped with an SA Peltier cooler (298 K - ΔT) and a Peltier heater (298 K + ΔT). Two microthermocouples (TCs) of 0.20 mm diameter were placed on the sample abreast of two electrodes connected to a Keithley 2400 source meter. The Seebeck coefficient was estimated by a linear fit to the measured ΔV vs. ΔT at different electrode spaces.

## Calculation of Interaction Energies

Pairwise interaction energies between PEDOT:PSS components and solvents are critical for elaborating molecular mechanism of solvent treatment in PEDOT:PSS. Pairwise interactions are calculated between solvents and components of PEDOT:PSS. The solvents include DMSO<sub>2</sub>, DMSO, EG and *N*-methyl pyrrolidone (NMP), while the components of PEDOT:PSS are neutral PEDOT trimer, polystyrene sulfonic acid trimer (PSSH), negatively charged PSS<sup>-</sup> trimer with one deprotonated PSS monomer, and positively charged radical PEDOT<sup>+</sup> trimer in the polaron state. Trimer structures were used for the PSS and the PEDOT, since it was experimentally determined that three PEDOT monomers possess one positive charge (Volkov et al., 2017). Initial structure pairs for density functional theory (DFT) calculations were determined by generating a large number of molecular configurations with excluded-volume constraints to determine energetically favorable configurations by employing statistical mechanics techniques (Fan et al., 1992). At least 12

lowest energy structures were determined for each of binary interactions between PEDOT and DMSO<sub>2</sub>. DFT calculations were performed by using M06-2X (Zhao and Truhlar, 2008) functional with 6-31+g(d) basis set in Gaussian16.A.03 software (Frisch et al., 2019). Both vacuum and implicit solvent methods for water are considered during the calculations. IEF-PCM implicit water continuum model is used to represent water solution (Tomasi et al., 2005).

## Free Energy of Solvation (ΔG<sub>sol</sub>) Calculations

Free energies of solvation (ΔG<sub>sol</sub>) were calculated for DMSO<sub>2</sub>, EDOT<sub>9</sub><sup>-3</sup> and SS<sub>18</sub><sup>-3</sup> solutes in DMSO, EG, tetrahydrofuran (THF), acetone, *N,N*-dimethyl formamide (DMF), NMP, CH<sub>2</sub>Cl<sub>2</sub>, hexane, MeOH and water solvents under periodic boundary conditions based on the coupling parameter method and thermodynamic integration algorithm (Figure S3) (Steinbrecher et al., 2011). The free energy of solvation was determined in three steps. Firstly, we computed the ideal free energy of solvation (ΔG<sub>id</sub>) by determining the free energy change associated with the discharge of the solute (DMSO<sub>2</sub>, EDOT<sub>9</sub><sup>-3</sup>, and SS<sub>18</sub><sup>-3</sup>) in vacuum. Then the neutral solute molecule was brought into contact with the solvent molecules; the free energy change for this step is called vdW free energy of solvation (ΔG<sub>vdw</sub>). Lastly, the solvated and discharged solute molecules are charged again in solvent to determine the electrostatic free energy of solvation (ΔG<sub>el</sub>) (Biovia, 2017). Total free energy of solvation (ΔG<sub>sol</sub>) was calculated as the sum of the free energy contributions from ideal, vdW and electrostatic free energies of solvation (Equation 1), noting that experimental densities were used for the solvents in free energy calculations.

$$\Delta G_{\text{sol}} = \Delta G_{\text{id}} + \Delta G_{\text{vdw}} + \Delta G_{\text{el}} \quad (1)$$

COMPASS (Condensed-Phase Optimized Molecular Potentials for Atomistic Simulation Studies) force field was used to validate solubility and phase properties of polymers in solution (Sun, 1998; Yildirim et al., 2015).

## RESULTS AND DISCUSSIONS

Figure 1 shows some common additives including DMSO, EG, NMP, and DMSO<sub>2</sub> used in the PEDOT:PSS for electrical conductivity enhancement. DMSO, EG, and NMP are in liquid forms at room temperature with high boiling point. During the process of film curing, high temperature has to be employed to vaporize these additives into ambient environment. To overcome this disadvantage, DMSO<sub>2</sub> is screened as a potential dopant. Unlike DMSO, EG and NMP, DMSO<sub>2</sub> is a solid and the sulfur atom in the molecule is at its highest oxidation state, making it more chemically stable. The fabrication process for PEDOT:PSS with DMSO<sub>2</sub> *via* drop-cast is shown in Figure 2, which is very similar to that of the commonly used DMSO, EG (Zhang et al., 2010) and other inorganic additives (Culebras et al., 2014a). It includes mixing PEDOT:PSS with additives, drop-cast of the solution onto the glass substrate and curing at a given temperature. When DMSO and inorganic acids are used

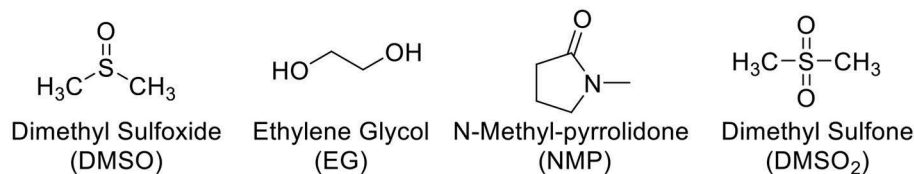


**FIGURE 1** | Chemical structures of different additives to PEDOT:PSS.

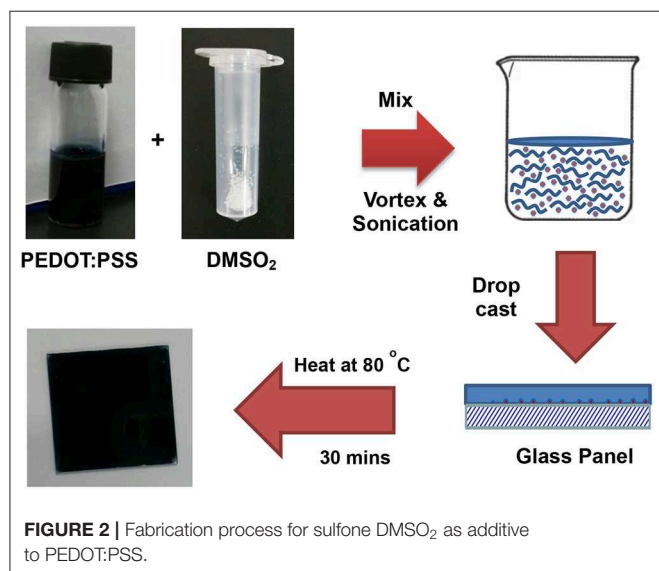


**FIGURE 2** | Fabrication process for sulfone DMSO<sub>2</sub> as additive to PEDOT:PSS.

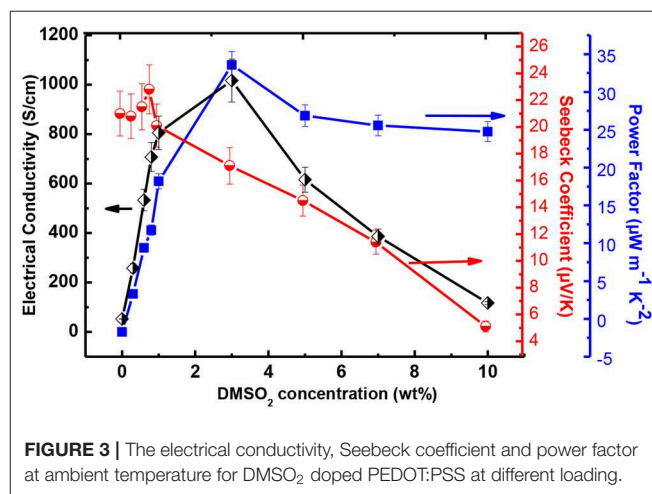


**FIGURE 3** | The electrical conductivity, Seebeck coefficient and power factor at ambient temperature for DMSO<sub>2</sub> doped PEDOT:PSS at different loading.

to dope PEDOT:PSS, a closed encasement or a fume-hood is required for the film preparation and curing process due to toxic and hazardous vapor caused by these volatile solvents. However, the processing and fabrication of solid DMSO<sub>2</sub> doped PEDOT films do not require a confined environment as no hazardous solvent vapor is produced. This opens up a new means to fabricate PEDOT:PSS films, which reduces the potential damage to human health and also lowers the fabrication cost. Similarly, electronic devices employing PEDOT:PSS and DMSO<sub>2</sub> as an additive would be much safer to consumers, particularly in the event that demands the stringent safety regulations such as wearable devices.

The thermoelectric performance in terms of electrical conductivity with respect to DMSO<sub>2</sub> concentration was measured and results are shown in **Figure 3**. The pristine PEDOT:PSS gave an electrical conductivity of 0.2 S/cm. With the increase in DMSO<sub>2</sub> loading, the electrical conductivity gradually increased and reached close to 1,100 S/cm. When over 3% additive loading was added, the decrease in electrical conductivity was observed, possibly due to the un-evenness of as-prepared film at high additive loading. Another plausible reason is that DMSO<sub>2</sub> play a somewhat insulation role if more loading of it applies, leading to the reduction in the electrical conductivity. This trend of electrical conductivity with respect to the amount of DMSO<sub>2</sub> added is very similar to known DMSO, EG, NMP and others dopants. Interestingly, the

electrical conductivity of PEDOT:PSS remained almost constant despite curing temperatures between 60–120°C, showing more advantages than processes using NMP or EG, which require a higher temperature and a much longer curing time to vaporize out the high boiling-point additives. The Seebeck coefficient was also measured and data are summarized in **Figure 3**. The Seebeck coefficient shows an overall decreasing trend with the increase of loading of DMSO<sub>2</sub>, and a highest Seebeck coefficient of 23 μV/K was achieved at 1% loading of DMSO<sub>2</sub>. The carrier concentration usually leads to a proportional increment of electrical conductivity. However, the Seebeck coefficient varies inversely due to the trade-off relationship between these two parameters. (Yao et al., 2010) The power factor increased sharply at a DMSO<sub>2</sub> loading of <3%. At a higher DMSO<sub>2</sub> loading, the power factor dropped. A highest power factor of 32 μW/mK<sup>2</sup> was obtained at 3% loading of DMSO<sub>2</sub>. The figure of merit (ZT) was approximately estimated to be 0.02 assuming that the thermal conductivity of PEDOT is 0.54 Wm<sup>-1</sup>K<sup>-1</sup> (Kyaw et al., 2017). The current ZT value is smaller than those reported (**Table S1**), but it is believed that it could be greatly improved if the further post-treatment that is able to reduce the doping level is performed to increase its Seebeck coefficient.

AFM and FESEM were used to understand the interaction between sulfone and PEDOT:PSS. AFM images were taken to observe the roughness for pristine and DMSO<sub>2</sub>-doped PEDOT:PSS films (**Figure 4**). Similar to the observation by Alshareef (Kumar et al., 2016), the rms roughness for pristine PEDOT:PSS is 1.8 nm (**Figure 4A**), showing very smooth and

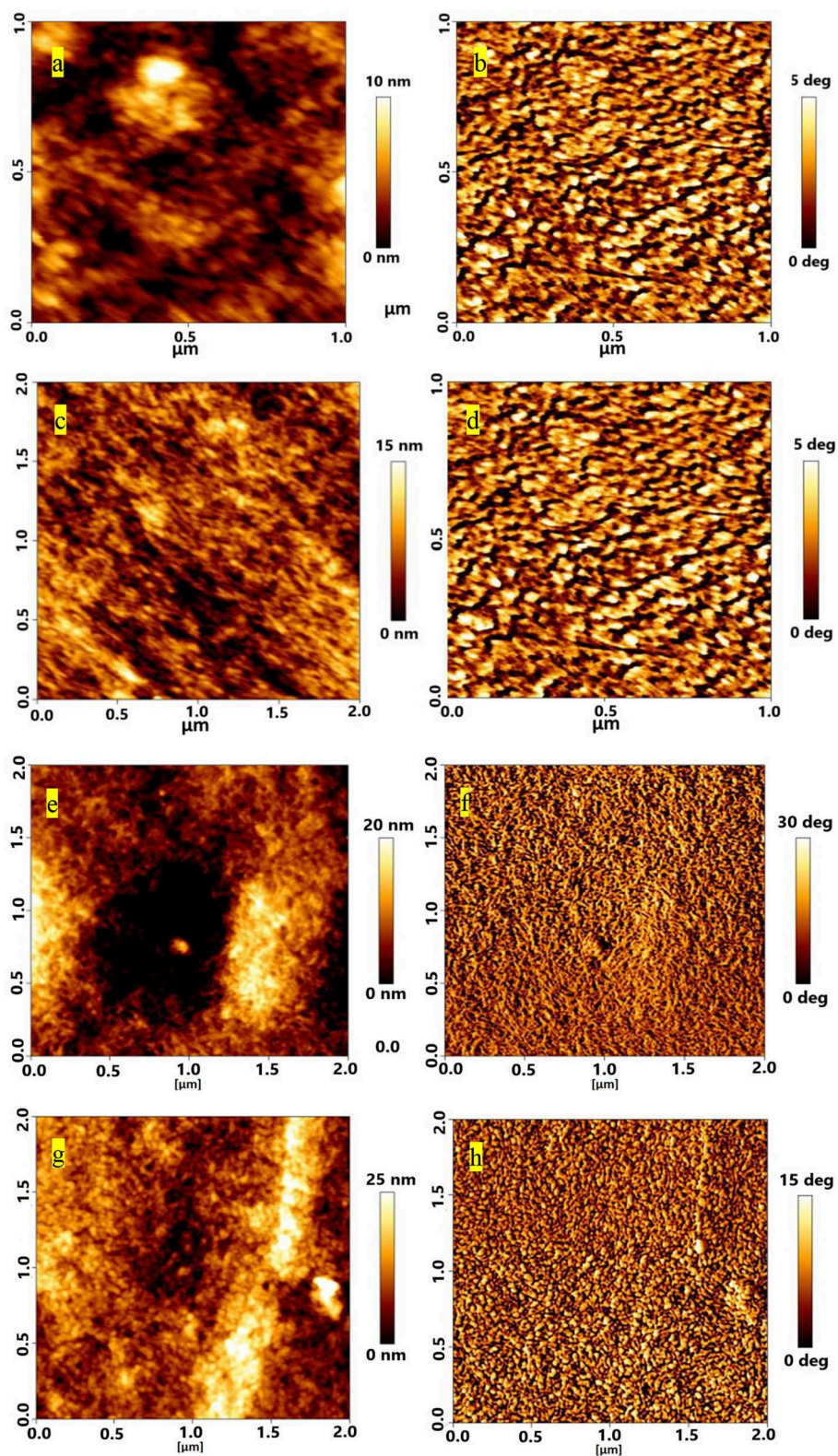


**FIGURE 4 |** AFM topography images of different loading of DMSO in PEDOT:PSS films for (a) pristine (c) 1% (e) 3% and (g) 5%; corresponding phase images are shown on right panels (b,d,f,h).

uniform film as prepared. Upon adding DMSO<sub>2</sub> into PEDOT:PSS at 1, 3, and 5% loading (Figures 4C,E,G), film roughness is ascending with the similar trend. At 1% loading (Figure 4C), the roughness was 4 nm with tiny fibrous structures observed by topography and phase images. Accordingly, 5.0 and 5.3 nm and 8.1 nm roughness were observed by careful examination on AFM images, showing that tiny crystal-like bright rods with regular shape was observed in their phase images (Figures 4B,D,F,H). The bright rods could be the uniform crystals which were formed by DMSO<sub>2</sub> during the curing process. Unlike conventional additives, such as liquid DMSO, EG, and NMP, DMSO<sub>2</sub> is in a solid form, and more chemically stable as the sulfur atom in DMSO<sub>2</sub> is fully oxidized.

FESEM images were used to examine the surface morphology for all the films doped with sulfone (Figure 5). Interestingly, a clear long fibrous structure embedded in the surface was found in the film prepared by 3% DMSO<sub>2</sub> in PEDOT:PSS. Such a long crystal structure helped well-orientation of the PEDOT:PSS backbone so that carriers can move in a more efficient way, resulting in higher electrical conductivity. In literature, three approaches have been used to enhance electrical conductivity of PEDOT:PSS. The first was the dedoping process through tuning the charge carrier concentration along the polymer chains. Bubnova et al. reported the use of tetrakis(dimethylamino)ethylene to tune the electron distribution along PEDOT:*p*-toluenesulfonate (PEDOT:Tos) to enhance electrical conductivity significantly (Bubnova et al., 2011; Tomlinson et al., 2015). The second approach is the secondary doping with organic solvents or counter-ions so as to tune the polymer chain conformation. For example, when DMSO or EG is employed in PEDOT:PSS solution, the strong Van der Waals interactions between the polar group of DMSO/EG and PEDOT:PSS chains can lead to a structural change from a benzoid to a quinoid structure in the polymer chains, resulting in a few magnitude of electrical conductivity enhancement (Jiang et al., 2008; Yue et al., 2012). The third approach is to remove the excess of insulation polymer, PSS, in the PEDOT:PSS system through post-treatment with DMSO, EG or acids (Kim et al., 2013). In contrast, in our DMSO<sub>2</sub> doped PEDOT:PSS system, the electrical conductivity enhancement is similarly due to the polymer alignment but induced by *in-situ* crystallization of solid DMSO<sub>2</sub> dopant as observed by microscopy images.

To further verify the polymer alignment of PEDOT:PSS induced by DMSO<sub>2</sub> crystallization, the X-ray diffraction (XRD) is used to check the diffraction of the pristine, DMSO<sub>2</sub>-doped PEDOT:PSS and pure DMSO<sub>2</sub> crystals (Figure 6). Four characteristic peaks:  $2\theta = 3.7^\circ$ ,  $6.6^\circ$ ,  $17.7^\circ$ , and  $26.0^\circ$  were observed on pristine sample which is consistent with the recent work published by Lee et al. (Kim et al., 2014) The low diffraction at  $3.7^\circ$ ,  $6.6^\circ$  and high diffraction at  $17.7^\circ$ , and  $26.0^\circ$  was attributed to the lamella stacking between two distinct alternate ordering PEDOT/PSS and inter-chain ring stacking between PEDOT:PSS, respectively. Due to the random orientation of polymer chains in the pristine PEDOT:PSS, it can be observed that much stronger diffraction at  $6.6^\circ$  than at  $3.7^\circ$  is observed, and the intensity ratio between the diffractions of  $6.6^\circ$  and  $3.7^\circ$  is 1.50. XRD shows that the diffraction at  $6.6^\circ$  is significantly reduced when DMSO<sub>2</sub>

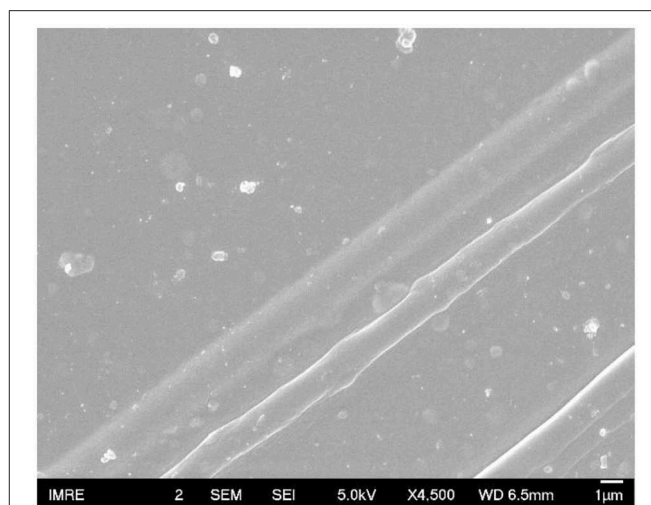


FIGURE 5 | FESEM micrograph of 3% DMSO<sub>2</sub> in PEDOT:PSS.

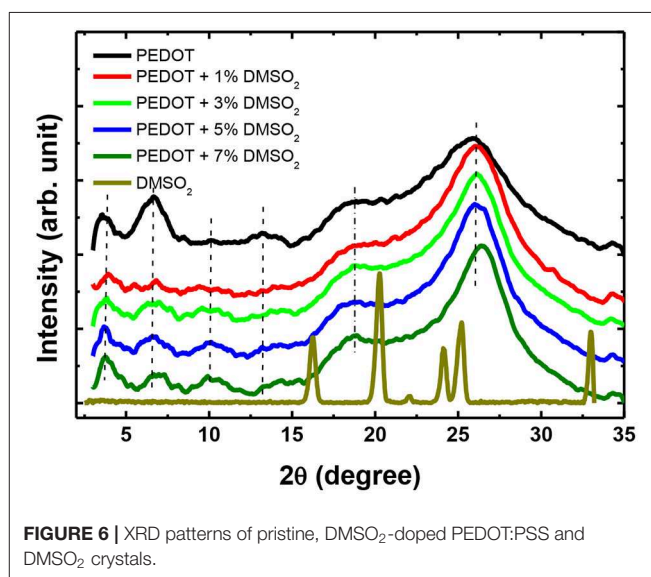
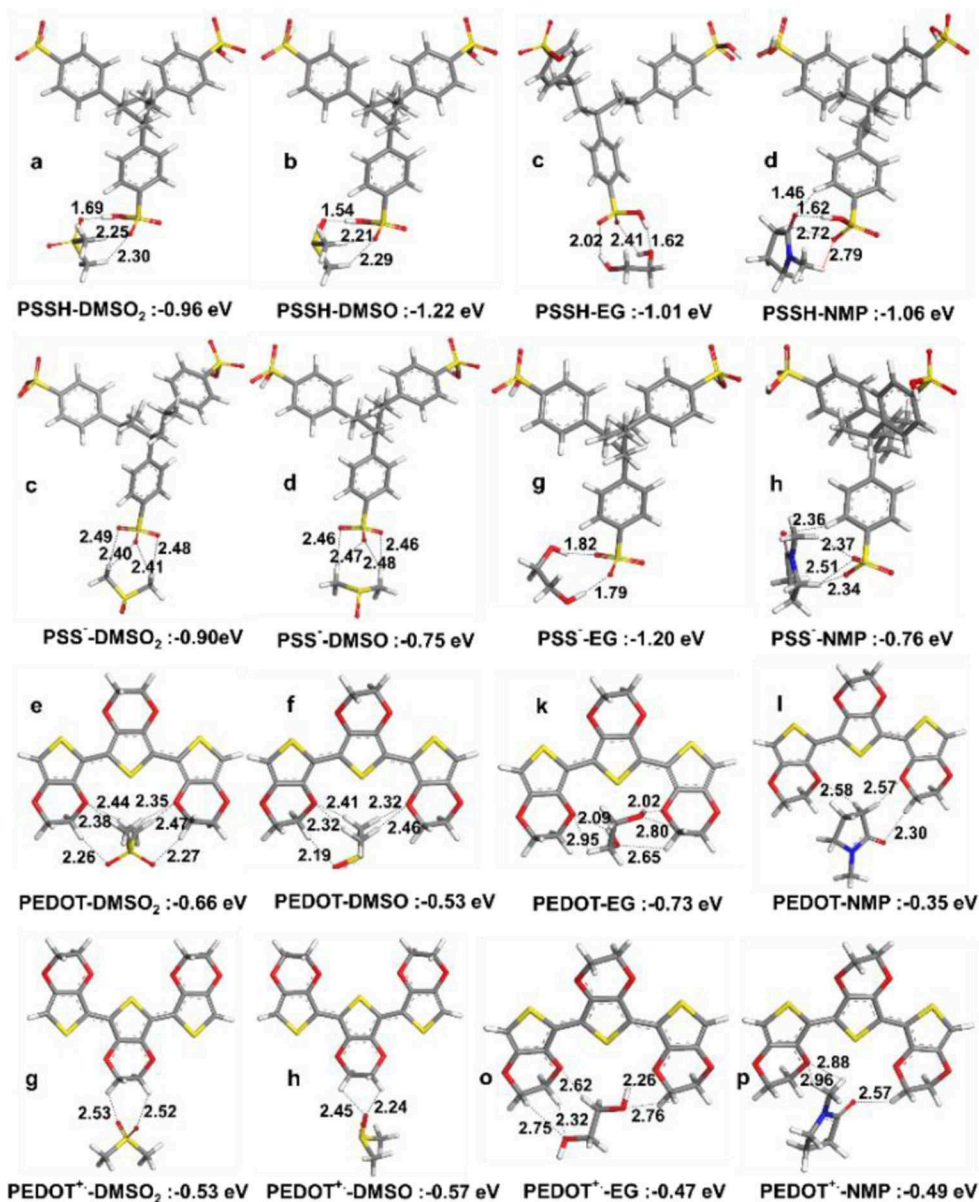


FIGURE 6 | XRD patterns of pristine, DMSO<sub>2</sub>-doped PEDOT:PSS and DMSO<sub>2</sub> crystals.

was loaded into PEDOT:PSS, while the diffraction at  $3.7^\circ$ ,  $17.7^\circ$ , and  $26.0^\circ$  remained relatively unchanged. More importantly, the intensity ratio between the diffraction of  $6.6^\circ$  and  $3.7^\circ$  become 0.49. This observation demonstrates that the polymers orient in a more ordered way toward one particular lamella stacking between the two distinct alternate ordering of PEDOT:PSS.

Meantime, the XRD diffraction patterns for pure DMSO<sub>2</sub> crystal are also measured for comparison. Characteristic diffraction peaks at  $17.2^\circ$ ,  $20.5^\circ$ ,  $24.0^\circ$ ,  $26.1^\circ$  and  $32.5^\circ$  were observed. However, when doped with PEDOT:PSS, no diffraction signals are observed indicating that the DMSO<sub>2</sub> crystal is wrapped by polymer chains, which is consistent with AFM studies (Figure 4). In other words, PEDOT:PSS is aligned in a more ordered manner, which is indirectly induced by DMSO<sub>2</sub> crystals wrapped by PEDOT:PSS.

Pairwise interaction energies were analyzed to explain observed enhancement in thermoelectric properties. Optimized



**FIGURE 7** | Optimized lowest energy structures and interaction energies in vacuum for (a–d) PSSH trimer with DMSO<sub>2</sub>, DMSO, EG, and NMP, (e–h) PSS<sup>-</sup> trimer with DMSO<sub>2</sub>, DMSO, EG and NMP, (i–l) PEDOT trimer with DMSO<sub>2</sub>, DMSO, EG, and NMP, (m–p) PEDOT<sup>+</sup> trimer with DMSO, DMSO<sub>2</sub>, EG, and NMP.

structures for the PSSH with DMSO<sub>2</sub>, DMSO, EG and NMP are given in **Figures 7A–D**, where interactions with the PSSH are found to follow the order of DMSO > DMSO<sub>2</sub> > NMP > EG. Hydrogen bonding is the main interactions, e.g., oxygen atoms in both DMSO and DMSO<sub>2</sub> would form hydrogen bonds with the –S–O–H in sulfonic acid group of the PSSH. In addition to strong hydrogen bonding, methyl hydrogens in DMSO and DMSO<sub>2</sub> interact and surround the two other sulfonate oxygen atoms in the PSSH, leading to the –SO<sub>3</sub>H groups in the PSSH to diminish interactions with other PSS and PEDOT chains. Therefore, separation of the excess insulating PSSH shell from the PSS<sup>-</sup> doped PEDOT<sup>+</sup> chains is believed to be a main mechanism. On the other hand, stronger hydrogen bonding interaction is

not possible between the deprotonated PSS<sup>-</sup> anion and DMSO and DMSO<sub>2</sub>, which consist mainly of relatively weaker –CH<sup>+</sup>–O<sup>-</sup> interaction. Hence, we found that the PSSH had much stronger interaction with all solvents compared to the PSS<sup>-</sup> except for EG; EG solvent can form two strong hydrogen bonds with the deprotonated PSS<sup>-</sup>. The difference in the solvation mechanism between EG and DMSO explains why big electrical conductivity enhancement was observed by co-solvent treatment in previous studies (Shi et al., 2015).

Neither PEDOT nor PEDOT<sup>+</sup> in the polaron state can form any hydrogen bonds with solvent molecules, and therefore their interactions with solvents are generally much weaker, where solvent molecules prefer to interact with oxygen atoms in the

dioxyethylene group (-OCH<sub>2</sub>CH<sub>2</sub>O-) and solvent oxygen atoms weakly interact with the -CH moieties of PEDOT. This implies that solvents are mainly interacting with the PSS shell, leaving the conductive PEDOT core to remain intact. The most important consequence here is that the lowest energy structures suggest similar enhancement mechanism and comparable performance for DMSO and DMSO<sub>2</sub>. The interactions are weaker than under water solvation effect, showing the advantage of post treatment compared to solution treatment.

For solvent interactions with single PSSH, PSSH-DMSO has stronger interaction compared to DMSO<sub>2</sub>. However, DMSO<sub>2</sub> with two oxygen atoms is bifunctional and thus is able to coordinate with two PSSH monomers (see **Figure 8** for solvent interactions). DMSO and DMSO<sub>2</sub> have higher interaction energies with the PSSH compared to EG and NMP. The difference among solvents is lowered under implicit water solvation effect for ternary interaction. According to the calculated interaction energies, the PSSH-solvent interaction can have two effects on the system, i.e., (i) chain expansion and phase separation of the PSSH shell as a result of decreasing PSS-PSS interactions, and (ii) charge screening and phase separation of PSS-PEDOT. Partial reduction of the excess PSSH shell that covers the conducting PEDOT components enhances the connectivity between PEDOT phases, directly resulting in the enhancement of electrical conductivity.

Based on AFM, FESEM, and XRD and theoretical studies, we propose a mechanism for electrical conductivity enhancement by DMSO<sub>2</sub> in **Figure 9**, illustrating a schematic for the role of DMSO<sub>2</sub> in doping PEDOT:PSS and polymer orientation arising from the crystallization. When water molecules slowly evaporate upon heating, the DMSO<sub>2</sub> concentration increases and thus its self-interaction leads to the formation of fibrous crystals. Such a fibrous structure triggers the alignment of long PSS chains resulting in well-orientation of PEDOT and better connection between PEDOT units absorbed to PSS chain to improve the electrical conductivity. In literature, it has well-reported that the PSS insulating polymer can be separated through DMSO, EG, or acid treatment (Culebras et al., 2014a; Park et al., 2014b).

Free energy of solvation calculations were performed in periodic cells for the PSS, PEDOT, and DMSO<sub>2</sub> solvation by organic solvents to understand the observed variation in structural and electrical conductivity properties (**Figure 10**). Since all the calculated solvation free energies are negative, mixing is expected in all cases. The highest  $|\Delta G_{\text{solv}}|$  is observed for the solvation of the PSS chain (across almost all solvents), proving that the mechanism of conductivity enhancement via the PSS phase separation. Hexane, which has the lowest  $|\Delta G_{\text{solv}}|$  around the PSS chain and DMSO<sub>2</sub> molecules, does not have any effect on the electrical conductivity and film thickness. THF and CH<sub>2</sub>Cl<sub>2</sub> solvents, which have high  $|\Delta G_{\text{solv}}|$  for PEDOT chains and good miscibility with the PSS chains, have low electrical conductivity and big thickness due to polymer expansion. The solvents that enhance electrical conductivity of PEDOT:PSS films treated with DMSO<sub>2</sub> should thus have high values of  $|\Delta G_{\text{solv}}|$  for either PSS solvation or DMSO<sub>2</sub> solvation. Besides, ideal solvent should have lower solvation free energy for PEDOT as a solute. As an example, DMSO can wash away insulating DMSO<sub>2</sub>

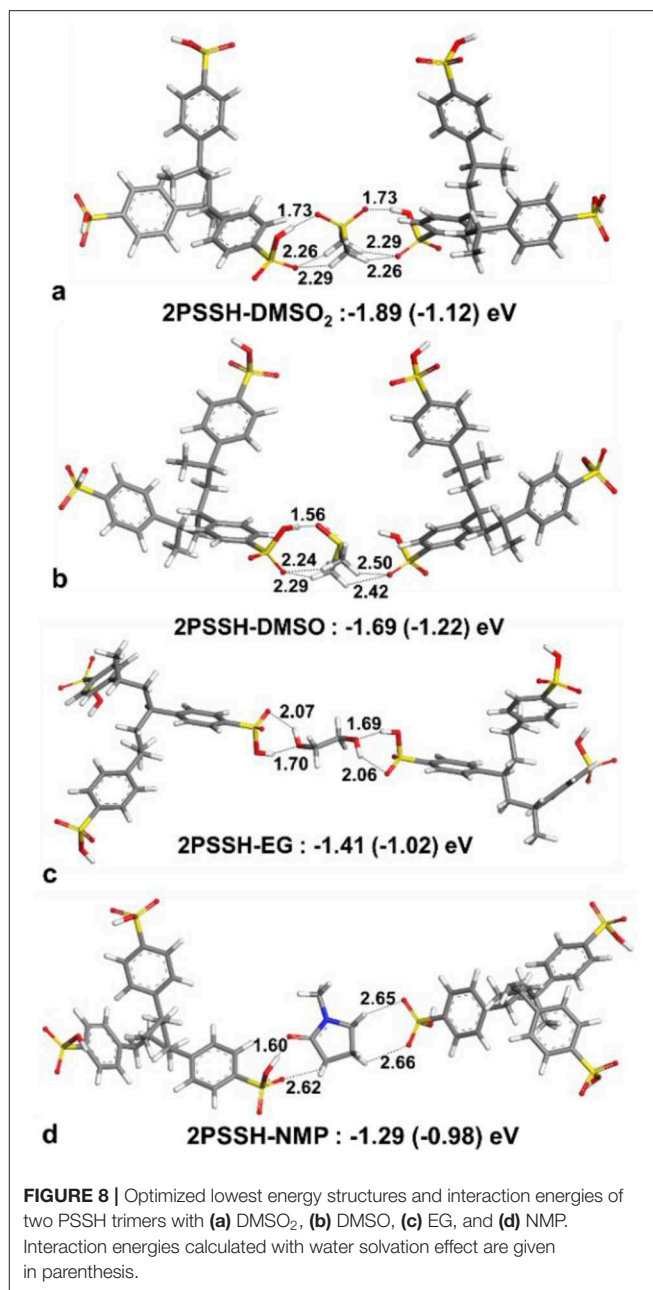
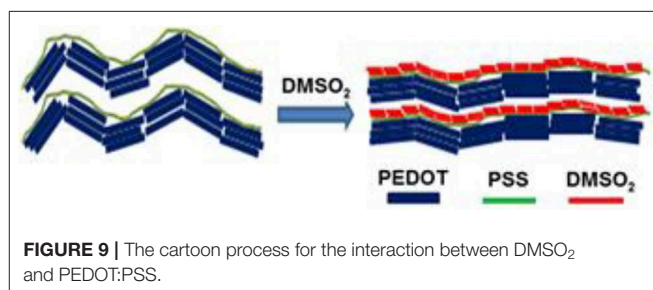


**FIGURE 8** | Optimized lowest energy structures and interaction energies of two PSSH trimers with (a) DMSO<sub>2</sub>, (b) DMSO, (c) EG, and (d) NMP. Interaction energies calculated with water solvation effect are given in parenthesis.



crystals in PEDOT:PSS, decrease thickness of films and enhance electrical conductivity. DMSO has similar electrical conductivity enhancement mechanism with DMSO<sub>2</sub>. That is the reason

why further electrical conductivity enhancement is limited. Acetone also have similar effect with strong solvation of DMSO<sub>2</sub>, decreasing thickness and slightly enhances the conductivity. Solvents that have strong solvation of both DMSO<sub>2</sub> and the PSS chains, such as EG and DMF should simultaneously decrease film thickness and enhance electrical conductivity. The mechanism of solvent interaction with the PSS chains is important so that secondary solvent with different interaction mechanism with the PSS chains compared to DMSO<sub>2</sub> can separate the remaining PSS chains to enhance conductivity further.

In order to obtain the electric properties of PEDOT:PSS films with different concentration of DMSO<sub>2</sub>, the Van der Pauw–Hall measurements were performed. **Table 1** lists the carrier mobility ( $\mu$ ), concentration ( $n$ ) and conductivity of PEDOT:PSS with DMSO<sub>2</sub>. The carrier mobility improved significantly with the increase of the concentration of additive in PEDOT:PSS film. It is reasonable to conclude that the enhancement in electric conductivity of PEDOT:PSS is due to the incorporation of DMSO<sub>2</sub>. The carrier concentration increases with the increase of additive concentrations but slightly decrease when the concentration of DMSO<sub>2</sub> is over 3%. As DMSO<sub>2</sub> does not behave

like a reducing agent to cause the change in the oxidation level of PEDOT. The increase in carrier concentration is probably due to the release of trapped carriers by polymer chains. DMSO<sub>2</sub> treatment induces the polymer alignment along a particular direction and thus pushes out the carriers from the polymer chains entangled with the PSSH. On the other hand, DMSO<sub>2</sub> with two oxygen atoms is bifunctional and thus is able to coordinate with two PSSH monomers. Based on the modeling (vide supra) partial reduction of the excess PSSH shell that covers the conducting PEDOT components enhances the connectivity between PEDOT phases, as a result, perhaps freeing more carriers and increasing the electric conductivity.

In addition, the long-term stability for our pre-mixed PEDOT:PSS and DMSO<sub>2</sub> solution is also investigated. Chemical de-doping with tetrakis(dimethylamino)ethylene, secondary doping with polar organic solvents like DMSO, EG and NMP have been used to obtain high electrical conductivity. However, it is known that most mixtures of PEDOT:PSS and solvent dopants cannot be stored for a long duration. **Figure 11** shows that pre-mixed solution of DMSO<sub>2</sub> and PEDOT:PSS can be stored at 2–6°C for up to 2 months without significant change of the electrical conductivity, benefiting many applications.

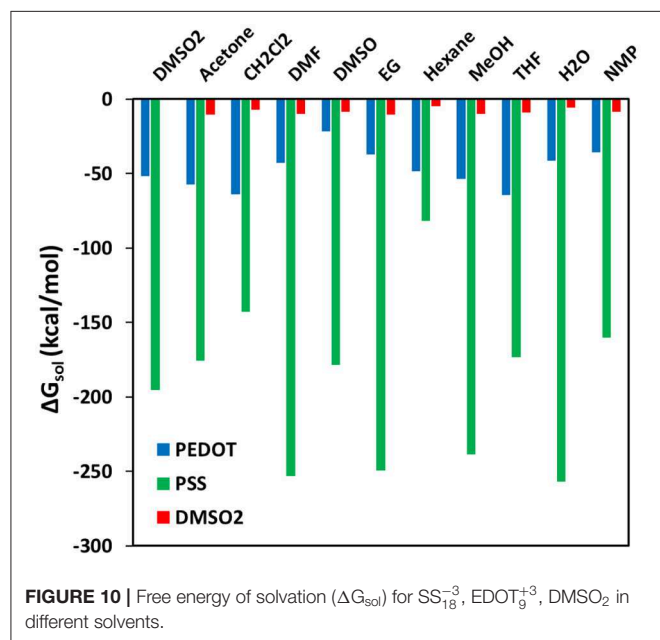


**FIGURE 10** | Free energy of solvation ( $\Delta G_{sol}$ ) for  $SS_{18}^{-3}$ ,  $EDOT_{9}^{+3}$ ,  $DMSO_2$  in different solvents.

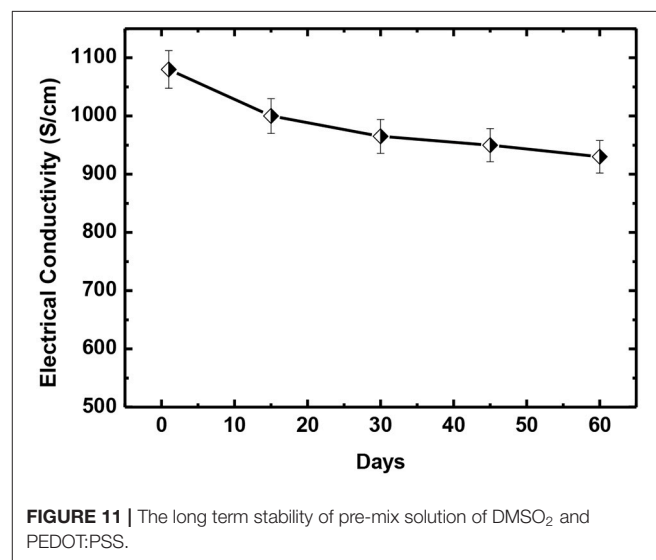


**FIGURE 11** | The long term stability of pre-mix solution of  $DMSO_2$  and PEDOT:PSS.

**TABLE 1** | Comparison of electric properties of PEDOT:PSS film with DMSO<sub>2</sub>.

Additive loading(%)	$\mu$ ( $cm^2/V\cdot s$ )	$n$ ( $cm^{-3}$ )	$\delta$ (S/cm)	Seebeck (S/cm)	PF ( $\mu\cdot W/mK^2$ )
0	$0.228 \pm 0.06$	$4.73 \pm 0.12 \times 10^{18}$	$0.2 \pm 0.1$	$21 \pm 0.17$	$0.006 \pm 0.001$
0.3	$1.14 \pm 0.1$	$4.83 \pm 0.22 \times 10^{20}$	$154 \pm 7$	$20.8 \pm 0.17$	$6.7 \pm 0.6$
0.6	$3.18 \pm 0.2$	$3.90 \pm 0.2 \times 10^{20}$	$340 \pm 217$	$21.5 \pm 0.17$	$15.7 \pm 1.4$
0.8	$7.88 \pm 0.3$	$2.45 \pm 0.22 \times 10^{20}$	$412 \pm 20$	$22.8 \pm 0.18$	$21.4 \pm 1.9$
1	$9.01 \pm 0.4$	$2.51 \pm 0.22 \times 10^{20}$	$609 \pm 30$	$20.1 \pm 0.16$	$24.6 \pm 2.2$
3	$10.391 \pm 0.5$	$2.82 \pm 0.22 \times 10^{20}$	$1080 \pm 50$	$17.1 \pm 0.13$	$31.5 \pm 2.8$
5	$10.221 \pm 0.5$	$2.49 \pm 0.22 \times 10^{20}$	$875 \pm 43$	$14.5 \pm 0.12$	$18.4 \pm 1.7$
7	$10.7 \pm 0.5$	$2.47 \pm 0.25 \times 10^{20}$	$835 \pm 42$	$11.4 \pm 0.1$	$10.9 \pm 0.9$

## CONCLUSION

As an alternative to conventional additives, DMSO<sub>2</sub> was identified as a dopant for the PEDOT: PSS to raise the electrical conductivity from 0.2 to 1080 S/cm with 3% loading. The enhancement in electrical conductivity is due to polymer alignment induced by crystallization of DMSO<sub>2</sub> in the PEDOT:PSS system. The modeling study revealed that the interactions at the molecular level demonstrated that DMSO<sub>2</sub> had comparable interaction energies with conventional solvents, which is responsible for conductivity enhancement. This new additive has an edge over other traditional dopants/additives as it is environmentally friendly, non-toxic, and has an easy doping process without additional treatment. Furthermore, PEDOT:PSS doped with DMSO<sub>2</sub> is stable and “green,” making it highly desired for industrial applications. DMSO<sub>2</sub> is unable to contribute to improvement in the Seebeck coefficient due to the inability of DMSO<sub>2</sub> to change the oxidation level of PEDOT. Our next step would be to introduce an additional post-treatment that enables to enhance the Seebeck coefficient, and thus leads to the high power factor of PEDOT.

## DATA AVAILABILITY STATEMENT

All datasets generated for this study are included in the article/**Supplementary Material**.

## REFERENCES

- Biovia, D. S. (2017). *BIOVIA Discovery Studio 2017 R2: A Comprehensive Predictive Science Application for the Life Sciences*. San Diego, CA. Available online at: <http://accelrys.com/products/collaborative-science/biovia-discovery-studio>
- Bubnova, O., Khan, Z. U., Malti, A., Braun, S., Fahlman, M., Berggren, M., et al. (2011). Optimization of the thermoelectric figure of merit in the conducting polymer poly (3, 4-ethylenedioxythiophene). *Nat. Mater.* 10, 429–433. doi: 10.1038/nmat3012
- Choi, J., Lee, J. Y., Lee, S. S., Park, C. R., and Kim, H. (2016). High-performance thermoelectric paper based on double carrier-filtering processes at nanowire heterojunctions. *Adv. Energy Mater.* 6:1502181. doi: 10.1002/aenm.201502181
- Choy, C. L. (1977). Thermal conductivity of polymers. *Polymer* 18, 984–1004. doi: 10.1016/0032-3861.90002-7
- Crispin, X., Jakobsson, F., Crispin, A., Grim, P., Andersson, P., Volodin, A., et al. (2006). The origin of the high conductivity of poly (3, 4-ethylenedioxythiophene)-poly (styrenesulfonate)(PEDOT-PSS) plastic electrodes. *Chem. Mater.* 18, 4354–4360. doi: 10.1021/cm061032+
- Culebras, M., Gomez, C., and Cantarero, A. (2014a). Enhanced thermoelectric performance of PEDOT with different counter-ions optimized by chemical reduction. *J. Mater. Chem. A* 2, 10109–10115. doi: 10.1039/C4TA01012D
- Culebras, M., Gómez, C. M., and Cantarero, A. (2014b). Review on polymers for thermoelectric applications. *Materials* 7, 6701–6732. doi: 10.3390/ma7096701
- Fan, C. F., Olafson, B. D., Blanco, M., and Hsu, S. L. (1992). Application of molecular simulation to derive phase diagrams of binary mixtures. *Macromolecules* 25, 3667–3676. doi: 10.1021/ma00040a010
- Feng, Z.-Q., Wu, J., Cho, W., Leach, M. K., Franz, E. W., Naim, Y. I., et al. (2013). Highly aligned poly (3, 4-ethylene dioxythiophene)(PEDOT) nano- and microscale fibers and tubes. *Polymer* 54, 702–708. doi: 10.1016/j.polymer.2012.10.057
- Frisch, M., Trucks, G., Schlegel, H., Scuseria, G., Robb, M., Cheeseman, J., et al. (2019). *Gaussian 16, Revision A*. Wallingford, CT: Gaussian, Inc.

## AUTHOR CONTRIBUTIONS

QZ, and JX conceived and designed the experiments. QZ, YZ, XW, and XS performed the experiments and contributed to the film fabrication, measurement, and data analysis. EY, TT, GW, and S-WY contributed to modeling and analysis. QZ, EY, and JX wrote and revised the paper.

## FUNDING

This work was financially supported by the Agency for Science, Technology and Research (A\*STAR), Industry Alignment Fund, Pharos Hybrid thermoelectric materials for ambient applications Program (Grant Nos.: 1527200019, 1527200021, and 1527200024).

## ACKNOWLEDGMENTS

The authors would like to acknowledge the support from the Institute of Materials Research and Engineering (IMRE), Agency for Science, Technology and Research (A\*STAR).

## SUPPLEMENTARY MATERIAL

The Supplementary Material for this article can be found online at: <https://www.frontiersin.org/articles/10.3389/fchem.2019.00783/full#supplementary-material>

- Han, S., Zhai, W., Chen, G., and Wang, X. (2014). Morphology and thermoelectric properties of graphene nanosheets wrapped with polypyrrole. *RSC Adv.* 4, 29281–29285. doi: 10.1039/C4RA04003A
- Hu, F., Cai, Q., Liao, F., Shao, M., and Lee, S.-T. (2015a). Recent advancements in nanogenerators for energy harvesting. *Small* 11, 5611–5628. doi: 10.1002/smll.201501011
- Hu, X., Chen, G., Wang, X., and Wang, H. (2015b). Tuning thermoelectric performance by nanostructure evolution of a conducting polymer. *J. Mater. Chem. A* 3, 20896–20902. doi: 10.1039/C5TA07381B
- Hu, Y., Shi, H., Song, H., Liu, C., Xu, J., Zhang, L., et al. (2013). Effects of a proton scavenger on the thermoelectric performance of free-standing polythiophene and its derivative films. *Synth. Met.* 181, 23–26. doi: 10.1016/j.synthmet.2013.08.006
- Jiang, F.-X., Xu, J.-K., Lu, B.-Y., Xie, Y., Huang, R.-J., and Li, L.-F. (2008). Condensed matter: electronic structure, electrical, magnetic, and optical properties: thermoelectric performance of poly (3, 4-ethylenedioxythiophene): poly (styrenesulfonate). *Chin. Phys. Lett.* 25, 2202–2205. doi: 10.1088/0256-307X/25/6/076
- Kaneko, H., Ishiguro, T., Takahashi, A., and Tsukamoto, J. (1993). Magnetoresistance and thermoelectric power studies of metal-nonmetal transition in iodine-doped polyacetylene. *Synth. Met.* 57, 4900–4905. doi: 10.1016/0379-6779(93)90836-L
- Kemp, N., Kaiser, A., Liu, C. J., Chapman, B., Mercier, O., Carr, A., et al. (1999). Thermoelectric power and conductivity of different types of polypyrrole. *J. Polym. Sci. Part B: Polym. Phys.* 37, 953–960.
- Kim, G. H., Shao, L., Zhang, K., and Pipe, K. P. (2013). Engineered doping of organic semiconductors for enhanced thermoelectric efficiency. *Nat. Mater.* 12, 719–723. doi: 10.1038/nmat3635
- Kim, J. Y., Kwon, M. H., Min, Y. K., Kwon, S., and Ihm, D. W. (2007). Self-Assembly And Crystalline Growth Of Poly (3, 4-Ethylenedioxythiophene) Nanofilms. *Adv. Mater. Weinheim.* 19, 3501–3506. doi: 10.1002/adma.200602163

- Kim, N., Kee, S., Lee, S. H., Lee, B. H., Kahng, Y. H., Jo, Y. R., et al. (2014). Highly Conductive PEDOT: PSS Nanofibrils Induced by Solution-Processed Crystallization. *Adv. Mater. Weinheim.* 26, 2268–2272. doi: 10.1002/adma.201304611
- Kumar, P., Zaia, E. W., Yildirim, E., Repaka, D. V. M., Yang, S.-W., Urban, J. J., et al. (2018). Polymer morphology and interfacial charge transfer dominate over energy-dependent scattering in organic-inorganic thermoelectrics. *Nat. Commun.* 9:5347. doi: 10.1038/s41467-018-07435-z
- Kumar, S. R. S., Kurra, N., and Alshareef, H. N. (2016). Enhanced high temperature thermoelectric response of sulphuric acid treated conducting polymer thin films. *J. Mater. Chem. C* 4, 215–221. doi: 10.1039/C5TC03145A
- Kyaw, A. K. K., Yemata, T. A., Wang, X., Lim, S. L., Chin, W. S., Hippalgaonkar, K., et al. (2017). Enhanced thermoelectric performance of PEDOT:PSS films by sequential post-treatment with formamide. *Macromol. Mater. Eng.* 303:1700429. doi: 10.1002/mame.201700429
- Laforgue, A., and Robitaille, L. (2010). Production of conductive PEDOT nanofibers by the combination of electrospinning and vapor-phase polymerization. *Macromolecules* 43, 4194–4200. doi: 10.1021/ma9027678
- Mateeva, N., Niculescu, H., Schlenoff, J., and Testardi, L. (1998). Correlation of Seebeck coefficient and electric conductivity in polyaniline and polypyrrole. *J. Appl. Phys.* 83, 3111–3117. doi: 10.1063/1.367119
- McGrail, B. T., Sehrioglu, A., and Pentzer, E. (2015). Polymer composites for thermoelectric applications. *Angew. Chem. Int. Ed.* 54, 1710–1723. doi: 10.1002/anie.201408431
- Moriarty, G. P., Briggs, K., Stevens, B., Yu, C., and Grunlan, J. C. (2013). Fully organic nanocomposites with high thermoelectric power factors by using a dual-stabilizer preparation. *Energy Technol.* 1, 265–272. doi: 10.1002/ente.201300018
- Park, G. O., Roh, J. W., Kim, J., Lee, K. Y., Jang, B., Lee, K. H., et al. (2014a). Enhanced thermoelectric properties of germanium powder/poly (3, 4-ethylenedioxythiophene): poly (4-styrenesulfonate) composites. *Thin Solid Films* 566, 14–18. doi: 10.1016/j.tsf.2014.07.011
- Park, H., Lee, S. H., Kim, F. S., Choi, H. H., Cheong, I. W., and Kim, J. H. (2014b). Enhanced thermoelectric properties of PEDOT: PSS nanofilms by a chemical dedoping process. *J. Mater. Chem. A* 2, 6532–6539. doi: 10.1039/C3TA14960A
- Park, T., Park, C., Kim, B., Shin, H., and Kim, E. (2013). Flexible PEDOT electrodes with large thermoelectric power factors to generate electricity by the touch of fingertips. *Energy Environ. Sci.* 6, 788–792. doi: 10.1039/c3ee23729j
- Shi, H., Liu, C., Jiang, Q., and Xu, J. (2015). Effective approaches to improve the electrical conductivity of PEDOT: PSS: a review. *Adv. Electron. Mater.* 1:1500017. doi: 10.1002/aelm.201500017
- Steinbrecher, T., Joung, I., and Case, D. A. (2011). Soft-core potentials in thermodynamic integration: comparing one- and two-step transformations. *J. Comput. Chem.* 32, 3253–3263. doi: 10.1002/jcc.21909
- Sun, H. (1998). COMPASS: An ab initio force-field optimized for condensed-phase applications overview with details on alkane and benzene compounds. *J. Phys. Chem. B* 102, 7338–7364. doi: 10.1021/jp980939v
- Timpanaro, S., Kemerink, M., Touwslager, F., De Kok, M., and Schrader, S. (2004). Morphology and conductivity of PEDOT/PSS films studied by scanning-tunneling microscopy. *Chem. Phys. Lett.* 394, 339–343. doi: 10.1016/j.cpllett.2004.07.035
- Tomasi, J., Mennucci, B., and Cammi, R. (2005). Quantum mechanical continuum solvation models. *Chem. Rev.* 105, 2999–3094. doi: 10.1021/cr9904009
- Tomlinson, E. P., Willmore, M. J., Zhu, X., Hilsmier, S. W., and Boudouris, B. W. (2015). Tuning the thermoelectric properties of a conducting polymer through blending with open-shell molecular dopants. *ACS Appl. Mater. Interfaces* 7, 18195–18200. doi: 10.1021/acsami.5b05860
- Volkov, A. V., Wijeratne, K., Mitraga, E., Ail, U., Zhao, D., Tybrandt, K., et al. (2017). Understanding the capacitance of PEDOT:PSS. *Adv. Funct. Mater.* 27:1700329. doi: 10.1002/adfm.201700329
- Wei, Q., Mukaida, M., Kirihara, K., Naitoh, Y., and Ishida, T. (2015). Recent progress on PEDOT-based thermoelectric materials. *Materials* 8, 732–750. doi: 10.3390/ma8020732
- Wu, J., Sun, Y., Pei, W.-B., Huang, L., Xu, W., and Zhang, Q. (2014). Polypyrrole nanotube film for flexible thermoelectric application. *Synth. Met.* 196, 173–177. doi: 10.1016/j.synthmet.2014.08.001
- Xu, K., Chen, G., and Qiu, D. (2013). Convenient construction of poly (3, 4-ethylenedioxythiophene)-graphene pie-like structure with enhanced thermoelectric performance. *J. Mater. Chem. A* 1, 12395–12399. doi: 10.1039/c3ta12691a
- Yao, Q., Chen, L., Zhang, W., Liufu, S., and Chen, X. (2010). Enhanced thermoelectric performance of single-walled carbon nanotubes/polyaniline hybrid nanocomposites. *ACS Nano* 4, 2445–2451. doi: 10.1021/nn1002562
- Yildirim, E., Wu, G., Yong, X., Tan, T. L., Zhu, Q., Xu, J., et al. (2018). A theoretical mechanistic study on electrical conductivity enhancement of DMSO treated PEDOT:PSS. *J. Mater. Chem. C* 6, 5122–5131. doi: 10.1039/C8TC00917A
- Yildirim, E., Zhang, Y., Lutkenhaus, J. L., and Sammalkorpi, M. (2015). Thermal transitions in polyelectrolyte assemblies occur via a dehydration mechanism. *ACS Macro Lett.* 4, 1017–1021. doi: 10.1021/acsmacrolett.5b00351
- Yoon, C., Reghu, M., Moses, D., Cao, Y., and Heeger, A. (1995). Transports in blends of conducting polymers. *Synth. Met.* 69, 255–258. doi: 10.1016/0379-6779(94)02439-6
- Yue, R., Chen, S., Liu, C., Lu, B., Xu, J., Wang, J., et al. (2012). Synthesis, characterization, and thermoelectric properties of a conducting copolymer of 1, 12-bis (carbazolyl) dodecane and thieno [3, 2-b] thiophene. *J. Solid State Electrochem.* 16, 117–126. doi: 10.1007/s10008-011-1292-0
- Zhang, B., Sun, J., Katz, H., Fang, F., and Opila, R. (2010). Promising thermoelectric properties of commercial PEDOT: PSS materials and their Bi<sub>2</sub>Te<sub>3</sub> powder composites. *ACS Appl. Mater. Interfaces* 2, 3170–3178. doi: 10.1021/am100654p
- Zhao, D., and Tan, G. (2014). A review of thermoelectric cooling: materials, modeling and applications. *Appl. Therm. Eng.* 66, 15–24. doi: 10.1016/j.applthermaleng.2014.01.074
- Zhao, Y., and Truhlar, D. G. (2008). The M06 suite of density functionals for main group thermochemistry, thermochemical kinetics, noncovalent interactions, excited states, and transition elements: two new functionals and systematic testing of four M06-class functionals and 12 other functionals. *Theor. Chem. Acc.* 120, 215–241. doi: 10.1007/s00214-007-0310-x

**Conflict of Interest:** The authors declare that the research was conducted in the absence of any commercial or financial relationships that could be construed as a potential conflict of interest.

Copyright © 2019 Zhu, Yildirim, Wang, Soo, Zheng, Tan, Wu, Yang and Xu. This is an open-access article distributed under the terms of the Creative Commons Attribution License (CC BY). The use, distribution or reproduction in other forums is permitted, provided the original author(s) and the copyright owner(s) are credited and that the original publication in this journal is cited, in accordance with accepted academic practice. No use, distribution or reproduction is permitted which does not comply with these terms.